Fast-Responding Bulk Hydrogels with Microstructure

WENSHENG CAI, RAM B. GUPTA

Department of Chemical Engineering, Auburn University, Auburn, Alabama 36849-5127

Received 22 December 2000; accepted 16 April 2001

ABSTRACT: A new method was used for the production of fast-responding bulk hydrogels with microstructure (BHMs) with a high swelling ratio. These BHMs were synthesized first by the formation of poly(*N*-isopropylacrylamide-*co*-acrylic acid) (NIPAAm–AA) microgel particles and then by the crosslinking of the particles with *N*-isopropylacrylamide monomer. The polymer obtained had the desired microstructure but was bulk (monolithic), so it could be used in a variety of applications. The NIPAAm–AA microgel particles were characterized with transmission electron microscopy, and the formed BHMs were characterized with scanning electron microscopy. Compared with conventional bulk hydrogels, the BHMs had very high swelling ratios and much faster swelling rates attributable to the collaboration of the ionized microgel particles and bulk hydrogels. An increase in the microgel particles embedded in the BHMs provided faster hydrogel swelling. The number of ionic acrylic acid groups in the hydrogels affected their swelling behavior. © 2002 John Wiley & Sons, Inc. J Appl Polym Sci 83: 169–178, 2002

Key words: hydrogel; microstructure; separation

INTRODUCTION

In the past 20 years, a considerable amount of research has been focused on polymer hydrogels that can undergo volume transitions in response to external physical or chemical stimuli such as pH,[1,2] pressure,[3,4] ionic strength,[5,6] electric field,[6] and temperature.[7,8] These materials have been studied extensively because of their applications in various technologies, including controlled drug release,[9,10] electrophoresis,[11] and bioseparation.[12,13] Among stimuli-sensitive hydrogels, poly(*N*-isopropylacrylamide) (PNIPAAm) is the most widely studied thermosensitive hydrogel; it undergoes a reversible volume phase transition at 32°C [lower critical solution temperature (LCST)].

For molecular separation applications, bulk hydrogels are needed in which swelling and shrinking are two important factors. Tanaka and Fillmore[14] reported that the hydrogel swelling rate is inversely proportional to the square of a linear dimension of the hydrogel. In general, bulk hydrogels take a long time to reach equilibrium swelling, from several hours to days, which is the main drawback for their practical usage. Therefore, attempts are being made to increase the swelling speed, and various synthesis methods have been suggested to prepare bulk hydrogels with fast responses and high swelling ratios.

Wu et al.[15] synthesized hydrogels with macroporous structures to increase the pore volume and surface area of bulk hydrogels for fast swelling/deswelling of PNIPAAm. They synthesized the hydrogels at temperatures above the LCST of the polymer by heating the reactor near the end of the polymerization. In addition, they added to the monomer solution another LCST monomer, hydroxypropyl cellulose, which worked as a pore-

Correspondence to: R. B. Gupta (gupta@auburn.edu).

Contract grant sponsor: U.S. Department of Energy; contract grant number: DE-FC36-99GO10417.

Journal of Applied Polymer Science, Vol. 83, 169–178 (2002)

forming agent, precipitating above its LCST (42°C). These hydrogels have larger pore volumes, larger average pore sizes, and faster macromolecular permeation rates in comparison with PNIPAAm synthesized by conventional methods. The macroporous PNIPAAm hydrogels have higher swelling ratios at temperatures below the LCST and exhibit faster deswelling and reswelling rates.

Comb-type grafted chains have been introduced to PNIPAAm backbones and crosslinked for rapid deswelling.[16] This comb-type grafted hydrogel has the same composition as conventional PNIPAAm but has a different architecture. The molecular mobility of the graft-type hydrogel is improved because of the freely mobile grafted chains. Higher equilibrium swellings at lower temperatures are observed for graft-type hydrogels than for normal hydrogels; longer graft chains result in higher equilibrium swelling because of the freely mobile grafted chains. These modified hydrogels can swell or deswell within 20 min. However, the swelling ratios are not improved in comparison with those of the PNIPAAm hydrogel.

Park and Park[17] and Chen et al.[18] synthesized hydrogels with super pores and open channels by introducing a gas into the monomer solutions during the polymerization. The formed hydrogel foams have gas cells, most of which are connected to form open channels. The size and number of the gas cell can be controlled by the monomer concentration, solution viscosity, crosslinking extent, surfactant, and type and amount of gas introduced into the polymerizing solution. The pore sizes in the superporous dried hydrogels are in the range of hundreds of micrometers. These hydrogel foams can fully swell within hours and can absorb more water than 100 times their own weight. However, the large pore size of the hydrogel restricts its application in some circumstances such as bioseparation processes, for which large pore sizes are not favorable because of the reduction in the separation efficiency.

Freeze drying and subsequent hydration in water are another way of accelerating the deswelling of PNIPAAm hydrogels. Using scanning electron microscopy (SEM), Kato and Takahashi[19] showed that the freeze-drying treatment made the hydrogel more porous, producing a weaker shrinking force, which made expansion easier compared with that of the conventional hydrogel.

Zhang and Zhou[20] synthesized PNIPAAm with water/acetone (1/1 v/v) as a mixed solvent during the hydrogel crosslinking reaction to obtain a faster deswelling rate. They proposed that during the polymerization process, the produced polymer chains were quite soluble and widely expanded in the mixed solvent. This may lead to the large swelling ratio of the hydrogel synthesized with mixed solvents. The swelling behaviors of the new hydrogel were not reported.

Hydrogels that have micrometer-level dimensions have also been synthesized, first by Standinger and Husemann,[21] and they were later named microgels by Baker.[22] Because microgel particle dimensions change upon shear, the microgels provide rheological control for automotive surface coatings. Microgels also show promise in pharmaceutical applications. The study of temperature- and pH-sensitive microgel particles has been an area of growing interest for a number of different applications.[23–26] The microgel particles have diameters ranging from 50 nm to 5 μm.[27] The bulk hydrogels need a long time to achieve full swelling, whereas a microgel particle can achieve a steady swelling state in less than a second when the temperature is changed because of its small size and large surface area. The rapid swelling/deswelling kinetics is one of the beneficial features of microgels in comparison with bulk hydrogels. More recently, researches have been able to combine the properties of two or more bulk hydrogels by forming interpenetrating polymer networks (IPNs), especially combining the pH and temperature sensitivities.[28,29] Inside IPN hydrogels, each network may retain its own properties, whereas the proportions of the networks are varied independently. The combined properties of the IPNs can be controlled by the ratios of their component monomers.

Temperature-sensitive hydrogels have been used to extract water and low molecular weight solutes from solutions to concentrate the macromolecules.[30–32] Most of these applications are limited PNIPAAm hydrogels, which can be pH- or temperature-sensitive and so can be regenerated with changes in the hydrogel pH or temperature for the release of absorbed water. In a comparison with traditional separation methods, such as distillation, in the chemical industry, the advantages of using thermosensitive hydrogels to extract solvents are obvious: these hydrogels can be easily regenerated by the temperature being raised above the LCST of the hydrogels, making the hydrogels release the absorbed water.

In the pulp and paper industry, the removal of water presents a major cost in manufacturing,

particularly water from in-process water streams, which mainly contain lignin and water (e.g., from white water cleaning, black-liquor spills, and oxygen-delignification filtration). The costs will increase greatly because of the enforcement of the new cluster rule legislation, which aims to reduce the load on waste treatment plants. Current methods of water removal such as evaporation are energy- and cost-intensive because of the large amount of energy needed for the evaporation for water. Hence, new approaches with lower energy and lower capital investment are needed.

In this article, we discuss the preparation of fast-responding bulk hydrogels with microstructure (BHMs). The swelling behavior of the new hydrogels is compared with that of conventional bulk hydrogels. The effects of the microgel particle loadings and the acrylic acid (AA) contents in the final BHMs on the swelling behavior are also studied. Finally, these BHMs are used to concentrate lignin (lignin hydrolytic and Indulin AT), blue dextran, and bovine serum albumin. Separation results are presented.

EXPERIMENTAL

Materials

N-Isopropylacrylamide (NIPAAm), *N,N′*-methylenebis(acrylamide) (BIS), ammonium persulfate (APS), and sodium metabisulfite (SBS) were all obtained from Aldrich Chemical Co. (Milwaukee, WI). Before AA (Aldrich Chemical) was used, the inhibitor was removed with inhibitor-remover packing (Aldrich Chemical). Buffer solutions with pH values of 3–10 were acquired from Fisher Scientific Co. (Houston, TX). Lignin hydrolytic [weight-average molecular weight (M_w) = 19,300 g/mol; Westvaco Chemical Co., Charleston Hgts., SC], Indulin AT (M_w = 2700 g/mol; Westvaco Chemical), blue dextran (M_w = 2,000,000 mol/g; Aldrich Chemical), and bovine serum albumin (M_w = 66,430 g/mol; Aldrich Chemical) were used as received.

Synthesis of the Microgel Particles

The microgel particles were synthesized by the surfactant free emulsion polymerization method.[33] Monomers NIPAAm and AA in the appropriate molar ratios were added into a 500-mL flask with a reflux condenser and a magnetic stirrer. The crosslinker (BIS) contents were kept at 2 wt % of the total monomer, and the total monomer concentrations were kept at 1 wt % of the solution. After the solution was purged with N_2 for half an hour, the initiator APS was added. The reaction temperature was maintained at 65°C. The reactions were allowed to proceed for 6–8 h, and the mixture was kept overnight at room temperature for completion of the reactions. Finally, the microgel solutions were concentrated under vacuum at room temperature to be used for further polymerization.

Characterization of the Microgel Particles

We used transmission electron microscopy (TEM) to observe the microgel particles. We prepared the TEM samples by placing a dilute drop of aqueous microgel particles onto the sample grid and allowing them to dry in air; the samples were observed under TEM (Zeiss EM 10CR; Carl Zeiss, Heidelberg, Germany).

Formation of the BHM

The NIPAAm monomer, microgel solution, and crosslinker BIS were mixed in a 50-mL, round-bottom bottle. The feed ratios of microgel particles to monomer were varied with changes in the concentration of the microgel solutions. The solution was shaken for 20 min for complete dissolution of the monomers and then purged with N_2 for 20 min for removal of the oxygen. Then, the redox initiators APS and SBS were added to the reaction mixture and polymerized at room temperature for 24 h. The formed bulk hydrogels were cut into disk form and put into ethanol to wash out the unreacted monomer, and the ethanol was changed every few hours during the washing process. Then, the hydrogels were vacuum-dried at 50–60°C for 1 day. The dried hydrogels were stored in a desiccator for further experiments. Conventional poly(*N*-isopropylacrylamide-*co*-acrylic acid) (NIPAAm–AA) bulk hydrogels were synthesized with a similar procedure, but without microgel. The NIPAAm–AA bulk hydrogel with *n* mol % AA in the feed ratio has been labeled NIPAAm–AA-*n*.

Characterization of the BHMs and Bulk Hydrogels

The surface structures of dry hydrogel pieces were examined via SEM. The hydrogel samples were first dried in a vacuum and coated with gold with a sputter coater (Pelco model Sc-7; Ted Pella, Inc., Redding, CA) for 60 s and then observed via SEM (Zeiss model DSM940; Carl Zeiss).

Differential Scanning Calorimetry (DSC) Analysis

DSC (Universal V2.5H TA Instrument; New Castle, DE) was used for the determination of the transition temperatures of the swelled hydrogels. Hydrogel pieces were first equilibrated at room temperature in pure water and then sealed into an aluminum pan. An empty aluminum sealed pan was used as a reference. In DSC, the sample was equilibrated at 10°C for 5 min and then heated to 55°C at rate of 2°C/min. The temperature corresponding to the maximum heat flow was taken as the LCST.

Measurement of the Swelling Capacity of the Hydrogels

The swelling ratios of the conventional bulk hydrogel and BHMs were measured as follows: a dried piece of hydrogel was placed in deionized water (pH $\sim$ 6.8) at a desired temperature for 1 day, the hydrogel swelled up to equilibrium, the hydrogel was taken out, surface water was removed with filter paper, and the weight of the wet hydrogel was recorded. The swelling ratio (SR) is defined as

$$\mathrm{SR} = (W_s - W_d)/W_d \tag{1}$$

where W_s is the weight of the wet hydrogel and W_d is the weight of the dry hydrogel.

Measurement of the Swelling and Deswelling Speeds of Hydrogels

The swelling and deswelling kinetics of bulk hydrogels and BHMs were measured gravimetrically at fixed temperatures. The extent of swelling was measured at different time intervals. The water uptake and water retention were calculated as indications of the response speed of the hydrogels:

$$W_U = 100*(W_t - W_d)/(W_e - W_d) \tag{2}$$

$$W_R = 100*(W_t - W_d)/(W_e - W_d) \tag{3}$$

where W_U is the water uptake percentage during swelling, W_R is the water retention percentage during deswelling, W_t is the weight of the gel at a particular time, W_d is the weight of the initial dry hydrogel, and W_e is the weight of the hydrogel at maximum swelling.

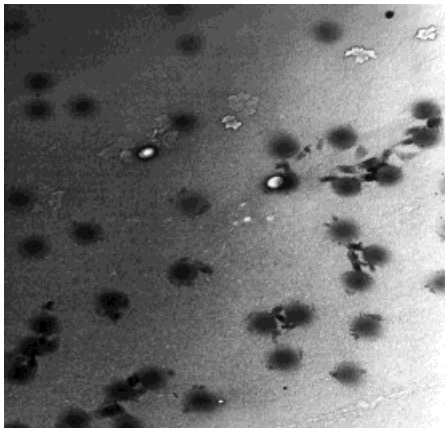

Figure 1 Transmission electron micrograph of NIPAAm–AA microgel particles (original magnification, 5000×).

Molecular Separation Experiments

In the separation experiments, various known amounts of dry hydrogel pieces were added to solutions to be concentrated at different temperatures (lignin hydrolytic and Indulin AT were dissolved in 0.01*N* NaOH, and blue dextran and bovine serum albumin were dissolved in water). The changes in the solution concentration before and after hydrogel contact were measured with an ultraviolet spectrophotometer (Spectronic Genesis 2; Spectronic Instruments, Rochester, NY). The separation efficiency (η) was defined as

$\eta = 100\times$ (measured concentration change/ maximum change expected from hydrogel swelling)

The maximum concentration change is based on the assumption that no macromolecule penetrates the hydrogel.

RESULTS AND DISCUSSION

Characterization of NIPAAm–AA Microgel Particles and NIPAAm–(NIPAAm–AA)$_{micro}$ BHM

Figure 1 is a TEM photograph of NIPAAm–AA microgel particles; here the particles are 500–700 nm. NIPAAm–AA microgels are ionic particles because of the carboxylic charge on AA. In these microgel particles, the AA groups tend to lie on the surface of the particles, and NIPAAm groups lie toward the inside; this prevents aggregation

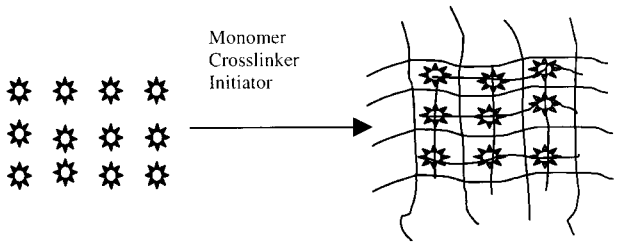

Figure 2 Schematic illustration of the formation of a BHM based on microgel particles.

between microgel particles and makes the microgel particles more stable in the aqueous solutions. In this conformation, the carboxyl groups on the microgel particle surface can also be further crosslinked under suitable conditions, forming interpenetrating network structures. Bouillot and Vincent[34] prepared poly(acrylic acid)/poly(acrylamide) (PAA/PAM) interpenetrating network particles. The second polymer, PAA, was synthesized in the presence of the first polymer, PAM microgel particles. Within the IPN microgel particles, there were cooperative interactions between the PAA and PAM chains, exhibiting sharp swelling transitions for the PAA/PAM particles. A higher swelling ratio was also observed above the upper critical solution temperature in comparison with the ratio for the poly(acrylic acid-*co*-acrylamide) copolymer microgel particles. On the basis of this ideal, we propose that when the monomer NIPAAm is mixed with the NIPAAm–AA microgel solution and crosslinker, the ionic microgel particles can be crosslinked with one another and into the bulk matrix, forming a BHM (Fig. 2).

Figure 3 shows SEM photographs of prepared

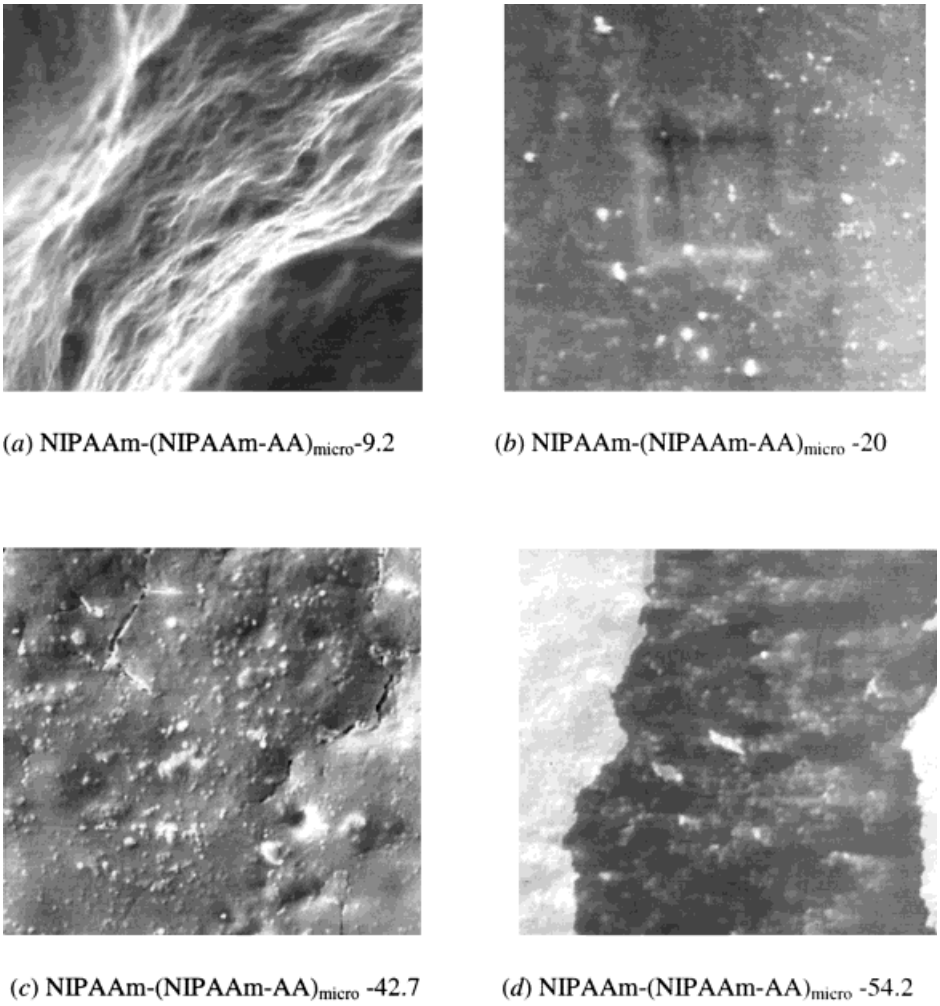

Figure 3 SEM photographs of NIPAAm–(NIPAAm–AA)$_{micro}$ with different amounts of the microgel [(a–c) original magnification, 2000×; (d) original magnification, 5000×].

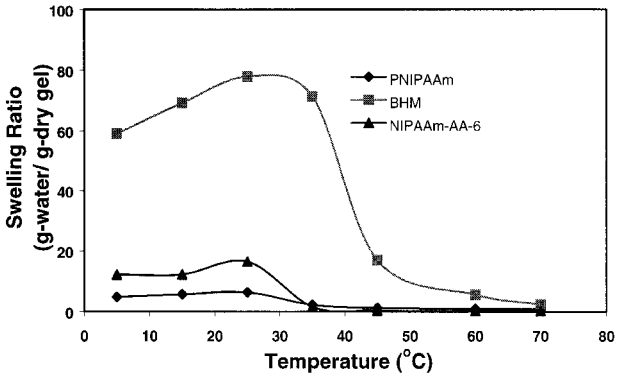

Figure 4 Effect of temperature on the swelling ratios of PNIPAAm and NIPAAm–AA-6 bulk hydrogels and NIPAAm–(NIPAAm–AA)$_{25}$ (40 wt% microgel).

NIPAAm–(NIPAAm–AA)$_{micro}$ BHMs with different NIPAAm–AA microgel contents. With an increasing feed ratio of the NIPAAm–AA microgel, more microgel particles are embedded into the matrix. When the feed ratio of the microgel is 9.2 wt %, few particles can be seen inside the matrix of the BHM; when the microgel amount in the feed ratio increases to 54.2 wt %, which is a majority of the volume in the BHM, a porous sponge structure is observed. The formed porous sponge structure indicates that the BHM has a more compatible network structure. Because this porous sponge structure is mainly composed of the microgel particles, which have fast a swelling rate when the temperature is changed, the BHM should display a fast response to external temperature changes.

Swelling Behavior of the BHMs and Bulk Hydrogels

The temperature dependence of the equilibrium swelling ratios of PNIPAAm and NIPAAm–AA-6 bulk hydrogels and NIPAAm–(NIPAAm–AA)$_{micro}$ BHM (40 wt % microgel particles) is illustrated in Figure 4. Both BHMs and bulk hydrogels are temperature-sensitive. From 5 to 25°C, these hydrogels have higher swelling ratios, suggesting that the hydrogen-bonding interactions between polymer chains and water are dominant at low temperatures. When the temperature is raised above the transition temperature, the hydrophobic interactions between the polymer chains become dominant and break the delicate balance between hydrogen-bonding and hydrophobic interactions, causing the hydrogel to collapse, decreasing the swelling ratio dramatically. Compared with the bulk hydrogels, the BHM shows much higher equilibrium swelling at room temperature. At 25°C, the BHM swelling ratio reaches 78, whereas both PNIPAAm and NIPAAm–AA-6 have swelling ratios below 20.

Figure 5 shows the swelling rate of the BHM and the PNIPAAm and NIPAAm–AA-6 hydrogels. The BHM swells much faster at room temperature. Within 5 h, it can swell to 80% of the maximum value, and within 10 h, the BHM swells to 90% of the maximum value; however, the PNIPAAm and NIPAAm–AA-6 bulk hydrogels only have 40% and 60% of their maximum water uptake, respectively, after 10 h of contact. The fast swelling rate of the BHM may be due to the collaborative interaction of both the microgel particles and the hydrogen-bonding interactions between the PNIPAAm matrix and water. When water enters the BHM network, the microstructures swell first, causing the whole interconnected matrix to swell afterward. This collaboration of the swelling of the ionized particles and bulk matrix enhances the swelling rate of the whole BHM matrix.

The deswelling behavior of hydrogels at 50°C is shown in Figure 6. Because 50°C is higher than the volume-transition temperature of the hydrogels, the three hydrogels release water sharply in the beginning and slowly later on. Because of the hydrophilicity of AA groups, NIPAAm–AA and BHM deswell slower than the PNIPAAm hydrogel. The BHM gives off 50% of its total water within 100 min.

pH Sensitivity

Figure 7 shows that both NIPAAm–(NIPAAm–AA)$_{micro}$ BHMs and NIPAAm–AA bulk hydrogel are pH-sensitive, whereas PNIPAAm is not. BHMs

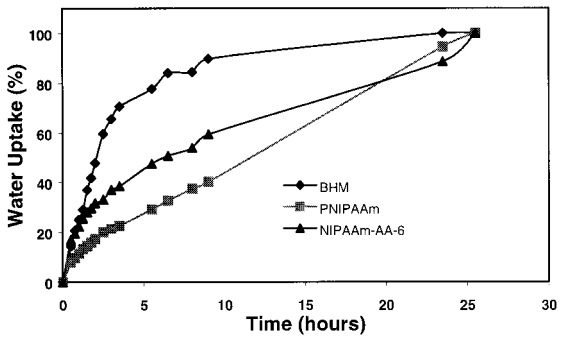

Figure 5 Comparison of the swelling kinetics of PNIPAAm and NIPAAm–AA-6 bulk hydrogels and NIPAAm–(NIPAAm–AA)$_{25}$ (40% microgel) at 23°C.

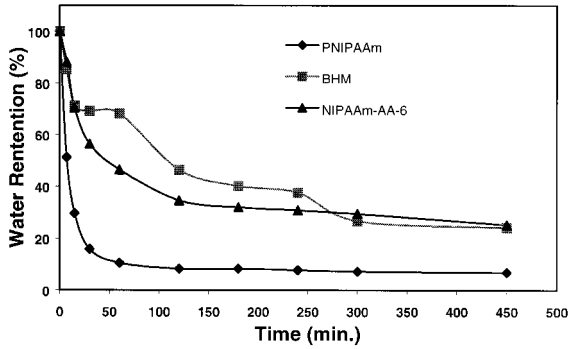

Figure 6 Deswelling speeds of PNIPAAm and NIPAAm–AA-6 bulk hydrogels and NIPAAm–$(NIPAAm–AA)_{25}$ (40% microgel) at 50°C.

reach maximum swelling at pH 8, after which the swelling decreases with an increase in the pH. The NIPAAm–AA bulk hydrogel does not show such a maximum within the experimental pH range. This difference in the pH sensitivity of the two hydrogels can be attributed to the different architectures of the acid groups in the hydrogels. In the BHM, all the acid groups lie on the surface of the microgel particles, and the NIPAAm molecular chains are linked through the active carboxyl groups, leading to the formation of the bulk hydrogel through microgel bridging. With an increase in the pH, more AA groups are ionized, and the electrostatic repulsion between the ionized groups results in a more expanded network. However, in high-pH solutions, the dissociated cations from the alkaline salt also increase, decreasing the ionic repulsion by shielding the ionic acid groups, and so the swelling decreases at a higher pH value. In BHMs, because all AA groups are in the microgel particles, they are easily

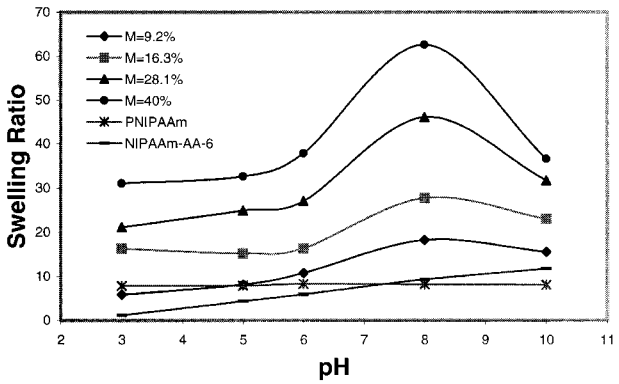

Figure 7 Swelling behavior as a function of pH at 23°C for PNIPAAm and NIPAAm–AA-6 bulk hydrogels and BHMs with different amounts of the microgel.

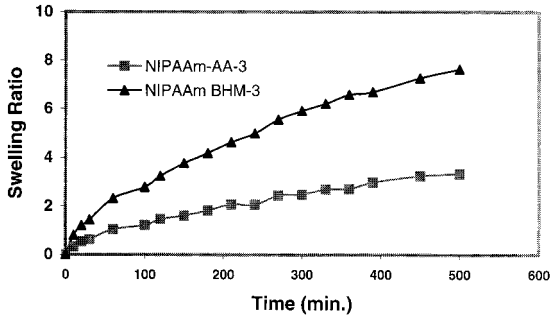

Figure 8 Swelling ratios of BHM and NIPAAm–AA bulk hydrogels with the same amount of AA.

shielded by the dissociated cations, causing a drop in the swelling at pHs higher than 8.

Effect of the AA Amount on the Swelling Behavior

Figure 8 confirms that the AA group architecture in the hydrogel plays an important role in the

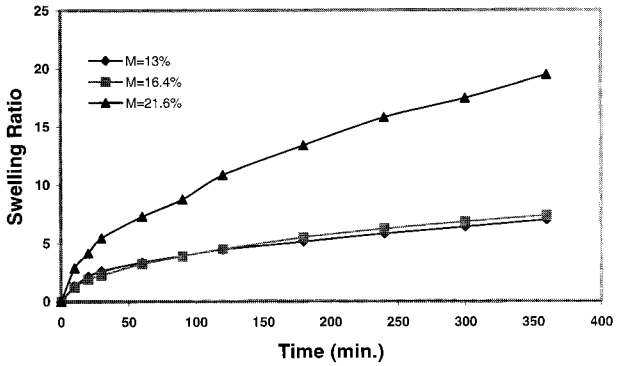

(a)

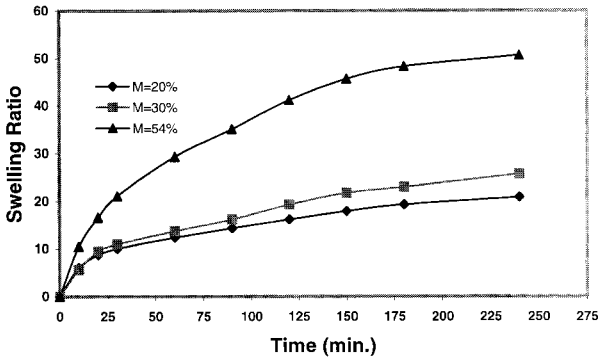

(b)

Figure 9 Effect of the amount of the microgel on the swelling behavior of the BHMs: (a) microgel NIPAAm–AA-15 and (b) microgel NIPAAm–AA-25.

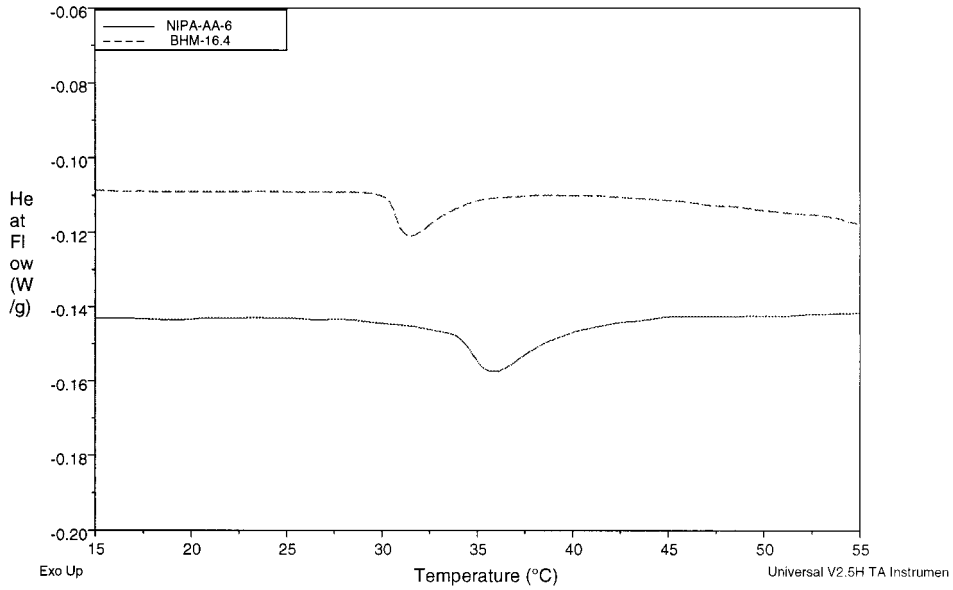

Figure 10 DSC diagrams of NIPAAm–AA-6 hydrogel and BHM (16.4 wt % microgel).

swelling behavior of hydrogels. In Figure 8, the swelling rates of the NIPAAM–(NIPAAm–AA)$_{micro}$ BHM and NIPAAm–AA-3 bulk hydrogel are compared; both are 3 wt % AA. Despite the small number of AA groups in the BHM, these groups greatly influence the swelling rate in comparison with the bulk hydrogel. The swelling rate of BHM is much faster than that of the NIPAAm–AA bulk hydrogel, which suggests that incorporating microgel particles accounts for the fast response of the BHM.

Effect of the Amount of the Microgel on the Swelling Behavior

The amount of the microgel particles in the BHM is very important for the swelling behavior (Fig. 9). A larger amount of the microgel in the hydrogel results in faster BHM swelling. When microgel contents are less than 20 wt %, the swelling ratio increases slowly, but when the microgel content is more than 30 wt %, there is a big increase in the swelling. This confirms that the swelling speed is mainly determined by the amount of the microgel in the BHM.

Thermal Analysis of the BHM and Bulk Hydrogel

The transition of the hydrogel in response to temperature changes can be observed with thermal analysis. Figure 10 shows DSC diagrams of the fully hydrated hydrogel of NIPAAm–AA-6 and the BHM containing 16.4 wt % microgel. The temperature corresponding to the maximum of the heat flow is defined as the LCST of the swollen hydrogel. With the incorporation of AA groups, the transition temperature of NIPAAm–AA-6 increases to 35.9°C, higher than the temperature for PNIPAAm (LCST = 33.8°C; not shown in Fig. 10). On the contrary, the transition temperature of the BHM is decreased to 31.4°C. This difference can be attributed to the different architectures of AA groups in the hydrogels. The transition enthalpy calculated from the peak areas are 12.57 and 12.80 J/g for NIPAAm–AA-6 and BHM, respectively. These values are different than the enthalpy of the PNIPAAm hydrogel transition, 14 J/g at a heating rate of 0.5°C/min.[35]

Separation of Macromolecules with BHMs

The concentration and recovery of solutes from dilute aqueous solutions are needed in the pharmaceutical, chemical, and environmental industries. Traditional separation methods, such as distillation and chromatography, are expensive. Hydrogel-based separation is promising because of the low energy costs. The separation is based on the absorption of water and low molecular weight solutes by the hydrogel, leaving behind a concentrated solution of larger molecules. The hydrogel is regenerated by being heated to its LCST, which usually is only slightly different from the current temperature.

Table I Separation of Lignin Hydrolytic with NIPAAM–(NIPAAm–AA)$_{micro}$ BHM Hydrogels After Contact for 24 h at 23°C

AA in the BHM (wt %)	Microgel in the BHM (wt %)	SR	η
0.85	16.4	26.2	12.6
1.67	16.6	25.6	13.7
2.55	13.0	34.4	51.0
3.61	16.3	40.8	47.2
6.14	28.1	72.2	33.6

Tables I and II show the separation results for lignin hydrolytic and Indulin AT with NIPAAm–(NIPAAm–AA)$_{micro}$ BHMs. Good separation efficiencies are achieved for both lignins. Both the AA and microgel contents affect the separation efficiency and swelling ratio. The swelling ratio increases with higher microgel contents in the BHM. For a given amount of the microgel, a larger amount of AA results in a higher swelling ratio and separation efficiency.

The NIPAAm–(NIPAAm–AA)$_{micro}$ BHM has a maximum separation efficiency for lignin hydrolytic and Indulin AT when the microgel content is 13 wt %. A higher content of the microgel in the BHM increases the swelling rate and ratio, but the separation efficiency decreases. For example, when the microgel content is 28.1 wt %, although the swelling ratios of the BHM in the lignin hydrolytic and Indulin AT are as high as 72.2 and 77.9, the separation efficiencies are only 33.6 and 40%, respectively.

Tables III and IV show the separation results for blue dextran and bovine serum albumin with the NIPAAm–(NIPAAm–AA)$_{micro}$ BHMs. Because both blue dextran and bovine serum albumin have larger molecular sizes than lignin molecules (M_w = 2,000,000 for blue dextran; M_w = 66,430 for bovine serum albumin) and the molecular attraction between the hydrogels and solutes is lower, the separation efficiencies are high. Also, a higher microgel content in the BHMs results in higher swelling. The separation efficiencies for blue dextran and bovine serum albumin are as high as 95.2 and 88.7%, respectively.

Table II Separation of Indulin AT with NIPAAM–(NIPAAm–AA)$_{micro}$ BHM Hydrogels After Contact for 24 h at 23°C

AA in the BHM (wt %)	Microgel in the BHM (wt %)	SR	η
0.85	16.4	22.6	42.4
1.67	16.6	35.0	51.8
2.55	13.0	34.6	75.1
3.61	16.3	38.7	64.6
6.14	28.1	77.9	40.0

Table III Separation of Blue Dextran with NIPAAM–(NIPAAm–AA)$_{micro}$ BHM Hydrogels After Contact for 24 h at 23°C

AA in the BHM (wt %)	Microgel in the BHM (wt %)	SR	η
0.85	16.4	18.3	65.2
1.67	13	15.8	72.7
3.61	16.3	37.7	95.2

CONCLUSION

A method for synthesizing BHMs has been developed. Compared with conventional hydrogels, the BHMs have a faster response along with a high swelling ratio and thermosensitivity. The faster response is due to the collaborative interactions between the ionized microgel particles and the bulk matrix. On contact with a solution, the microgel particles swell first, causing the overall bulk matrix to swell quickly. Because of their high absorption capacity and temperature sensitivity, the BHMs can be used to efficiently concentrate or separate macromolecules. Separations are demonstrated with NIPAAm–(NIPAAm–AA)$_{micro}$ BHMs to concentrate lignin hydrolytic, Indulin AT, blue dextran, and bovine serum albumin in aqueous solutions.

Table IV Separation of Bovine Serum Albumin with NIPAAM–(NIPAAm–AA)$_{micro}$ BHM Hydrogels After Contact for 24 h at 23°C

AA in the BHM (wt %)	Microgel in the BHM (wt %)	SR	η
0.85	16.4	35.5	88.7
1.67	13.0	71.3	73.6
3.61	16.3	72.7	54.7

REFERENCES

1. Hirotsu, S.; Hirokawa, Y.; Tanaka, T. J Chem Phys 1987, 87, 1392.
2. Dong, L. C.; Hoffman, A. S. J Controlled Release 1990, 13, 21.
3. Zhang, X.; Wang, Y. X.; Wang, S. C. Chem Eng Sci 1996, 51, 3235.
4. Wang, K. L.; Burban, J. H.; Cussler, E. L. Adv Polym Sci 1993, 110, 67.
5. Markland, P.; Zhang, Y.; Amidon, G. L.; Yang, V. C. J Biomed Mater Res 1999, 47, 595.
6. Tanaka, T.; Nishio, I.; Sun, S. T.; Ueno-Nishio, S. Science 1982, 218, 467.
7. Hirokawa, Y.; Tanaka, T. AIP Conf Proc (Phys Chem Porous Media) 1984, 107, 203.
8. Gotoh, T.; Nakatani, Y.; Sakohara, S. J Appl Polym Sci 1998, 69, 895.
9. Okana, T.; Bae, Y. H.; Kim, S. W. J Controlled Release 1989, 9, 271.
10. Hoffman, A. S.; Afrassiabi, A.; Dong, L. C. J Controlled Release 1986, 4, 213.
11. Liu, L.; Li, P. S.; Asher, S. A. Nature 1999, 397, 141.
12. Jin, M. R.; Wu, C. F.; Lin, P. Y.; Hou, W. J Appl Polym Sci 1995, 56, 285.
13. Sun, Y. S.; Qiu, Z. Y.; Hong, Y. L. Chin J Polym Sci 1992, 10, 311.
14. Tanaka, T.; Fillmore, D. J. J Chem Phys 1979, 70, 1214.
15. Wu, B. S.; Hoffman, A. S.; Yager, P. J Polym Sci Part A: Polym Chem 1992, 30, 2121.
16. Kaneko, Y.; Sakai, K.; Kkuchi, A.; Yoshida, R.; Sakurai, Y.; Okano, T. Macromolecules 1995, 28, 7717.
17. Park, K.; Park, H. U.S. Pat. 5,750,585 (1998).
18. Chen, J.; Park, H.; Park, K. J Biomed Mater Res 1999, 44, 53.
19. Kato, N.; Takahashi, F. Bull Chem Soc Jpn 1997, 70, 1289.
20. Zhang, X. Z.; Zhou, R. X. Eur Polym J 2000, 36, 643.
21. Standinger, H.; Husemann, E. Ber Dtsch Chem Ges 1935, 68, 1618.
22. Baker, W. O. Ind Eng Chem 1949, 41, 51.
23. Nair, M.; Tan, J. S. U.S. Pat. 5,078,994 (1992).
24. Nair, M.; Lobo, L. A.; Osburn, T. K. U.S. Pat. 6,001,549 (1999).
25. Renfrew, J. A.; Waterhouse, P.; Stevens, J. K. U.S. Pat. 5,627,022 (1997).
26. Tsuchiya, Y.; Tobinaga, K. U.S. Pat. 5,200,461 (1993).
27. Pelton, R. Adv Colloid Interface Sci 2000, 85, 1.
28. Zhang, J.; Peppas, N. A. Macromolecules 2000, 33, 102.
29. Girard-Reyder, E.; Pascault, J. P. Macromolecules 2000, 33, 3084.
30. Cussler, E. L. U.S. Pat. 4,828,701 (1989).
31. Cussler, E. L. U.S. Pat. 4,555,344 (1985).
32. Johnson, D. W.; Cussler, E. L.; Trank, S. J. U.S. Pat. 4,863,613 (1989).
33. Pelton, R. H.; Chibante, P. Colloids Surf 1986, 20, 247.
34. Bouillot, P.; Vincent, B. Colloid Polym Sci 2000, 278, 74.
35. Grinberg, N. V.; Dubovik, A. S.; Grinberg, V. Y.; Kuznetsov, D. V.; Makhaeva, E. E.; Grosberg, A. Y.; Tanaka, T. Macromolecules 1999, 32, 1471.